Non-Hermitian higher-order Weyl semimetals

Sayed Ali Akbar Ghorashi, Tianhe Li, and Masatoshi Sato

Non-Hermitian Higher-Order Weyl Semimetals

Sayed Ali Akbar Ghorashi,[1, 2, *] Tianhe Li,[3] and Masatoshi Sato[4]

[1] *Department of Physics, William & Mary, Williamsburg, Virginia 23187, USA*
[2] *Department of Physics and Astronomy, Stony Brook University, Stony Brook, NY 11794, USA*
[3] *Department of Physics and Institute for Condensed Matter Theory,*
University of Illinois at Urbana-Champaign, IL 61801, USA
[4] *Yukawa Institute for Theoretical Physics, Kyoto University, Kyoto 606-8502, Japan*
(Dated: October 19, 2021)

We study non-Hermitian higher-order Weyl semimetals (NHHOWSMs) possessing real spectra and having inversion $\mathcal{I}$ ($\mathcal{I}$-NHHOWSM) or time-reversal symmetry $\mathcal{T}$ ($\mathcal{T}$-NHHOWSM). When the reality of bulk spectra is lost, the NHHOWSMs exhibit various configurations of surface Fermi arcs and Exceptional Fermi Rings (EFRs), providing a setup to investigate them on an equal footing. The EFRs only appear in the region between $2nd$-order Weyl nodes. We also discover Weyl nodes originating from non-Hermicity, called *non-Hermitian Weyl nodes (NHWNs)*. Remarkably, we find $\mathcal{T}$-NHHOWSMs which host only $2nd$-order NHWNs, having both surface and hinge Fermi arcs protected by the quantized biorthogonal Chern number and quadrupole moment, respectively. We call this intrinsically non-Hermitian phase *exceptional HOWSM*. In contrast to ordinary Weyl nodes, the NHWNs can instantly deform to line nodes, forming a *monopole comet*. The NHWNs also show *exceptional tilt-rigidity*, which is a strong resistance towards titling due to attachment to exceptional structures. This phenomenon can be a promising experimental knob. Finally, we reveal the exceptional stability of Fermi arcs called *exceptional helicity*. Surface Fermi arcs having opposite chirality can live on the same surface without gapping out each other due to the complex nature of the spectrum. Our work motivates an immediate experimental realization of NHHOWSMs.

Introduction.–Non-Hermitian and higher-order topological phases are two new branches of topological phases which have ignited numerous attentions over the last few years [1–35]. Recently, the interplay of these two have also been studied [36–49]. However, despite attempts to understand the role of non-Hermiticity in systems having higher-order topology the effect of non-Hermitian perturbation has yet remains to be explored in 3d higher-order semimetals. Very recently we have studied the non-Hermitian higher-order Dirac semimetals (NHHODSMs) [50].

In this letter, we consider the the effect of C_4-symmetric non-Hermitian perturbations on the higher-order Weyl semimetals (HOWSMs) [51]. We find $\mathcal{I}$ and $\mathcal{T}$ symmetric models that possess real bulk spectrum up to a critical strength of non-Hermiticity while respecting anti-PT symmetry. We show that, when the complexity emerge, these models can host a novel classes of non-Hermitian Weyl nodes (NHWNs) that are intrinsic to Non-Hermitian systems. We characterize these new WNs using biorthogonal Chern number and a new 1D winding number. Both $\mathcal{I}, \mathcal{T}$-symmetric models feature various configurations of coexisting real and NHWNs in bulk as well as surface Fermi Arcs (FAs) and exceptional Fermi Rings (EFRs) that are protected by symmetries of class $\mathcal{P}$AI [52]. Interestingly, the $\mathcal{T}$ symmetric model additionally host real hinge FAs having quantized biorthogonal quadrupole moments and protected by C_4^z symmetry, exhibiting a unique Non-Hermitian higher-order Weyl semimetal (NHHOWSMs). Strikingly, we find that by gaping out all the real WNs, a novel and genuinely non-Hermitian Weyl phase, dubbed as *exceptional HOWSM*, emerges which hosts only $2nd$-order NHWNs. Furthermore, we reveal some distinct properties of NHWNs. First, we show that unlike the real WNs they can be destabilized in presence of a Hermitian perturbations such that they can instantly deform to a novel nodal line structure which we dubbed, *monopole comet*, where while maintaining their monopole charges, they connect on the surface FAs at original position of NHWNs (head of comet). Second, interestingly, we show that some classes of NHWNs exhibit strong resistance towards tilting due to presence of ESs in compare to their real counterparts. A phenomenon that we call *exceptional tilt-rigidity* and can be used as a promising experimental probe/knob. Finally, we reveal a remarkable phenomenon that we call it *exceptional helicity* in which surface band connectivity can be altered while removing EFRs in a way that FAs having opposite chirality live in the same surface without gapping out each other. Fig. 1 summarizes some of the main results of our work.

$H_w^{\mathcal{I}}$ *Model.*—We start by the following $\mathcal{I}$-symmetric non-Hermitian model,

$$H_w^{\mathcal{I}} = H_{HODSM}^{\mathcal{I}}(\mathbf{k}) + im_1\Gamma_0 a_0(\mathbf{k}) + \alpha\sigma_0\kappa_2 \quad (1)$$

where $H_{HODSM}(\mathbf{k}) = \sum_{i=1}^{4} a_i(\mathbf{k})\Gamma_i$ [54], $a_4(\mathbf{k}) = \left(\gamma + \frac{1}{2}\cos k_z + \cos k_x\right)$, $a_3(\mathbf{k}) = \sin(k_x)$, $a_2(\mathbf{k}) = \left(\gamma + \frac{1}{2}\cos k_z + \cos k_y\right)$, $a_1(\mathbf{k}) = \sin(k_y)$, and γ represent the intra-cell coupling. $\{\Gamma_\alpha\}$ are direct products of Pauli matrices, σ_i, κ_i, following $\Gamma_0 = \sigma^3\kappa^0, \Gamma_i = -\sigma^2\kappa^i$ for $i = 1, 2, 3$, and $\Gamma_4 = \sigma^1\kappa^0$, $a_0(\mathbf{k}) = (\cos(k_x) - \cos(k_y))$ and m_1 is a real constant. The amplitudes of inter-cell hoppings is set to 1, and we will work in the C_4^z symmet-
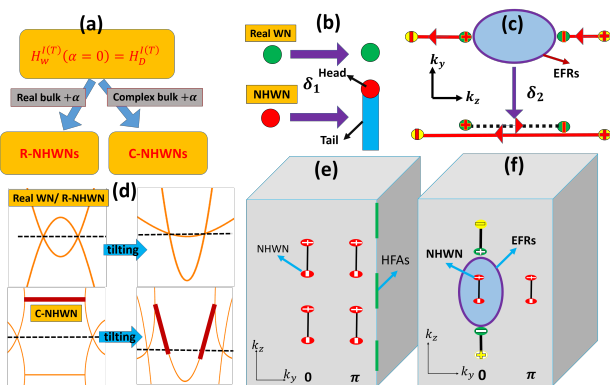
FIG. 1. Summary of main results.(a) Upon the addition of α to non-Hermitian Dirac semimetallic phase of [50]($H_w^{\mathcal{I}(\mathcal{T})}(\alpha = 0)$) having real (complex) spectrum the R-NHWNs (C-NHWNs) can appear aside from the real WNs of Hermitian limit. (b) An example of instability of NHWNs in the bulk: in presence of the perturbation δ_1 they deform to a intrinsically non-Hermitian nodal line structure, *monopole comet*, that while maintaining their original monopole charge, they are connected on the surface only via the original position of un-deformed NHWNs (head of comet) [see Fig. 4(c) for the surface plot]. (c) The surface instability of EFRs: in presence of the perturbation δ_2 they deform by changing band connectivity of surface FAs generating a region of counter-propagating FAs a phenomenon that we dubbed *exceptional-helicity.*[WNs shifted for visibility] (d) *Exceptional tilt-rigidity*: The C-NHWNs show strong resistance towards tilting due to ESs (red bars) in compare to real WNs and R-NHWNs. (e) *Exceptional NHHOWSMs*: A genuinely non-Hermitian class of $\mathcal{T}$-NHHOWSMs which host only NHWNs of higher-order topology i.e, all the nodes are connected both through the surface *and* hinge. (f) An example of surface configuration in $H^{\mathcal{I}}$, where EFRs and surface FAs overlap. Similar configurations are possible for $H^{\mathcal{T}}$, while it can host HFAs as well. For more surface configurations see Figs. 2,3.

ric limit. For $\alpha = 0$ but $m_1 \neq 0$ the Eq. (1) represent a NHDSM phase which shows real anti-PT symmetric bulk hosting Dirac nodes while the surface is PT symmetric and complex. The surface become complex by developing EFRs connecting the projections of two Dirac nodes on the surface and as a result the original hinge FAs of H_{HODSM} gap out. On the other hand, for $\alpha \neq 0$, $m_1 = 0$, H_w^I is a $\mathcal{I}$-HOWSM which can host a pair of $1st$-order or $2nd$-order WNs or combination of both types of WNs [51]. The $2nd$-order WNs are defined as the transition point between a phase having non-zero Chern number to the one having quantized quadrupole moment (q_{xy}). Therefore, they show coexistence of surface and C_4^z symmetry protected hinge FAs. When both m_1 and α are non-zero, the bulk is still anti-PT symmetric but chiral symmetry and combination of reciprocity and $\mathcal{I}$ are broken, hence $H_w^{\mathcal{I}}$ belongs to the class $\mathcal{PC}^\dagger$ of non-Hermitian topological phases[52].

Similar to non-Hermitian Dirac semimetallic phases in

[50], interestingly, the bulk spectrum remains real up to a critical value of m_1. The spectrum of Eq. (1) can be obtained as $E_{\pm,\pm}(\mathbf{k}) = \pm\sqrt{f(k) + \alpha^2 \pm 2\alpha\sqrt{g(k)}}$, where $f(k) = \sum_i^4 a_i^2(\mathbf{k}) - m_1^2 a_0^2(\mathbf{k})$ and $g(k) = a_2^2(\mathbf{k}) + a_4^2(\mathbf{k}) - m_1^2 a_0^2(\mathbf{k})$. At $(k_x, k_y) = (0, \pi), (\pi, 0)$, $a_1 = a_3 = 0$, interestingly, when $\sqrt{a_2^2(\mathbf{k}) + a_4^2(\mathbf{k}) - m_1^2 a_0^2(\mathbf{k})} - |\alpha| = 0$ a new set of WNs may emerge coexisting with real WNs and are located at $\cos(k_z) = -2\gamma \pm \sqrt{2}\sqrt{4m_1^2 + \alpha^2 - 2}$. This is particularly interesting as heuristically addition of non-Hermitian perturbations to Weyl/Dirac nodes results in deformation of the nodes to exceptional rings[1, 35, 55]. Here, on the other hand, NHWNs are indeed point-like nodes. We call these new nodes *Non-Hermitian Weyl nodes (NHWNs)* and we will show that while they share some common properties with real WNs, they behave distinctly in presence of an external Hermitian perturbations. Interestingly, NHWNs can appear in two types. If we start with a NHDSM phase having real (complex) spectra, the emergent NHWNs can be detached (attached) to bulk exceptional structures (ESs) and henceforth and we denote them as R-NHWNS (C-NHWNs) [53].

Now let us investigate the surface. Fig. 2, shows the evolution of x-surface states [y-surface is identical] as tuning the α for a fixed value of m_1 [56]. By increasing α from zero the real bulk Dirac nodes split. On the surface, interestingly, the EFRs survive only between two $2nd$-order WNs, where in the limit of $m_1 = 0$ shows $q_{x,y} = 0.5$ Fig.2(a). This is because, phenomenologically, the EFRs emerge by removing hinge FAs, which means that when $H^{\mathcal{I}}$ hosts only $1st$-order WNs the EFRs do not appear, indicating an intimate interplay of non-Hermitian and higher-order topology. The real WNs ($1st$ and $2nd$-order) similar to the Hermitian limit are connected by conventional surface FAs, providing a platform that hosts both the conventional FAs and EFRs at different momenta.

When the NHWNs appear, their projections on x-surface connect at both $k_y = 0, \pi$ and form a region where the EFRs and surface FAs overlap (Fig. 2(b,e)). Then, as α increases, through series of surface phase transitions, the EFRs gaps out between NHWNs and only survive in the region between the $2nd$-order and NHWNs (note they have same monopole charges) Fig. 2(c). By further increasing of α the NHWNs exchange their positions with $2nd$-order WNs, but in doing so, they exchange their band connectivity at $k_y = 0$ through a surface phase transition in a way that instead each NHWNs connects to real $1st$-order WNs Fig. 2(d) and all EFRs are gapped out.

The x-surface possess PT symmetry while the bulk respects anti-PT symmetry then all the models discussed in this work, present another examples of 3D higher-order *hybrid-PT topological phases* [50]. The topological protection of EFRs can be understood as follows. On the x-surface, only the $\mathcal{T}\mathcal{M}_y\mathcal{M}_z$ is preserved and hence ac-
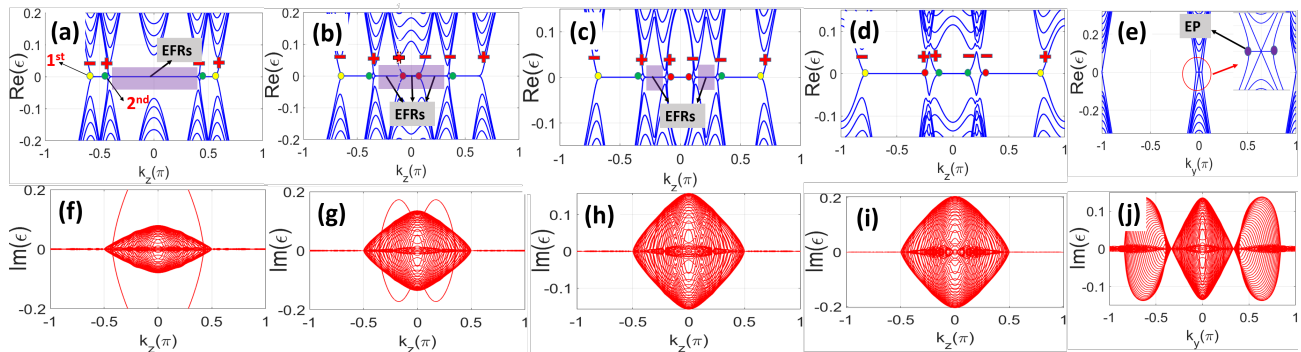
FIG. 2. (a-d) The real part of x-surface [1 OBC] along $k_z(k_y = 0)$ for $H^{\mathcal{I}}$ having $\gamma = -1, m_1 = 0.78$ and $\alpha = 0.2, 0.35, 0.42, 0.6$, respectively. (e) The corresponding cut along $k_y(k_z = 0)$ for (b). (f-j) The imaginary counterparts of (a-e). The yellow, green, red dots and purple shade denote the $1st$, $2nd$-order, NHWNs and EFRs, respectively. See [53] for plots of their corresponding $k_y = \pi$ cut and the bulk spectrum.

cording to [52], it belongs to class $\mathcal{P}$AI of gapless non-Hermitian topological phases. As a result, the EFRs on the surface are protected by a $\mathbb{Z}_2$ topological number[57]. $H_w^{\mathcal{T}}$ *Model.*—We consider the following $\mathcal{T}$-symmetric model,

$$H_w^{\mathcal{T}} = H_{HODSM}^{\mathcal{T}}(\mathbf{k}) + im_2\Gamma_0 a_0(\mathbf{k})\sin(k_z) + \alpha\sigma^0\kappa^2\sin(k_z) \quad (2)$$

similar to Eq. (1), $H_w^{\mathcal{I}}$ belongs to the class $\mathcal{P}$C† and preserves anti-PT, even though it has a broken $\mathcal{I}$ symmetry. For $\alpha = 0$, $H^{\mathcal{T}}$ represents a $\mathcal{T}$-NHHODSM. On the other hand, in the Hermitian $m_2 = 0$ limit, Eq. (2) is a $\mathcal{T}$-HOWSM. Due to $\mathcal{T}$, the minimum number of all the WNs are four. Therefore, on each of $(0, \pi)$ and $(\pi, 0)$ axes, at some finite vale of α four NHWNs emerge. As a result on the surfaces, there are two separate patches of EFRs separated by a real gap. Here, again, we observe that EFRs can only appear in the region between two real $2nd$-order WNs. Remarkably, by further opening boundary along the x and y-directions to get a hinge, we find hinge FAs (HFAs) that survive in a region corresponding to the gapped region of the surface states 3(a,e). However, by further increasing of α, the EFRs can be removed and like the Hermitian limit, the HFAs are connected to $2nd$-order 3(b,f). Strikingly, by removing all the real WNs via decreasing γ, we obtain a $\mathcal{T}$-NHHOWSM that possess hinge FAs both in the middle and at the end of BZ 3(c,d,g). This means all the NHWNs are of $2nd$-order type and so are connected both through surface and hinges. This is in sharp contrast to the parent Hermitian $\mathcal{T}$-HOWSMs which only two out of four WNs are $2nd$-order. We emphasize that this is a novel HOWSM which is intrinsic only to the NH phases as the NHWNs can only exist in presence of NH perturbation. We call this new phase *exceptional higher-order Weyl semimetal*. In order to characterize the zero-mode at the hinges, we employ a biorthogonal [9, 58] real-space formula [59–61]

for quadrupole moment, q_{xy}^{LR}, which is shown to correctly capture the higher-order topology in NHHODSMs [50]. As is evident in the case of exceptional HOWSMs, for the regions having C_4^z symmetry protected hinge FAs the $q^{LR} = 0.5$ (see Fig. 3(h)). *Topological charges of WNs.*— We use two methods to characterize the topological character of WNs. First, we obtain the monopole charge of each WNs by computing the biorthogonal real-space formula of Chern number ($\mathcal{C}^{LR}$) at each 2D k_z-slice [8, 62] (e.g., see Fig. 3(h)). Second, we introduce a new 1D winding number. Using the fact that each of $k_y = 0, \pi$ ($k_x = 0, \pi$) planes separately respect the sublattice symmetry (even though the full 3D Hamiltonian of $H_w^{\mathcal{I},\mathcal{T}}$ do not), $H_w^{\mathcal{I},\mathcal{T}}$ can be block-off diagonalized at $k_x = 0, \pi$ ($k_y = 0, \pi$) planes having $\mathcal{Q}_{1,2}$ blocks. Note that, in general for non-Hermitian systems $Q_2 \neq Q_1^\dagger$. Therefore, we define a new k_z-dependent 1D winding number as following,

$$w_{l,(1,2)}(k_z) = \int_{-\pi}^{\pi} \frac{1}{2\pi i}\partial_{k_x}\ln\det[Q_{(1,2)}] \quad (3)$$

where $l = k_y = 0, \pi$. Interestingly, by tuning the k_z the w_l changes by ± 1 as crossing any WNs. We emphasize that this is general and can detect both the real and (C,R)-NHWNs. The total $w_l = w_{l,1} + w_{l,2}$ are zero. However, the difference $\bar{w}_l = (w_{l,2} - w_{l,1})/2$ are non-zero and quantized to ± 1. Fig. 4(a), shows the $\bar{w}_l$ for $k_y = 0, \pi$. For the real WNs on the $k_x = 0$ cut, $\bar{w}_0$ is consistent with the monopole charges of $\pm$. However, interestingly, the NHWNs at $(0, \pi)$ and $(\pi, 0)$ carry opposite winding numbers. Therefore, their sum $w = w_0 + w_\pi$ is zero but their difference reflects the Chern number $\bar{w} = \bar{w}_0 - \bar{w}_\pi$.

Stability of NHWNs.—Let us now investigate the stability of NHWNs introduced in this work. The Hermitian/real WNs and their corresponding surface FAs are stable and only can be gapped or deformed through a topological phase transition. On the other hand, here
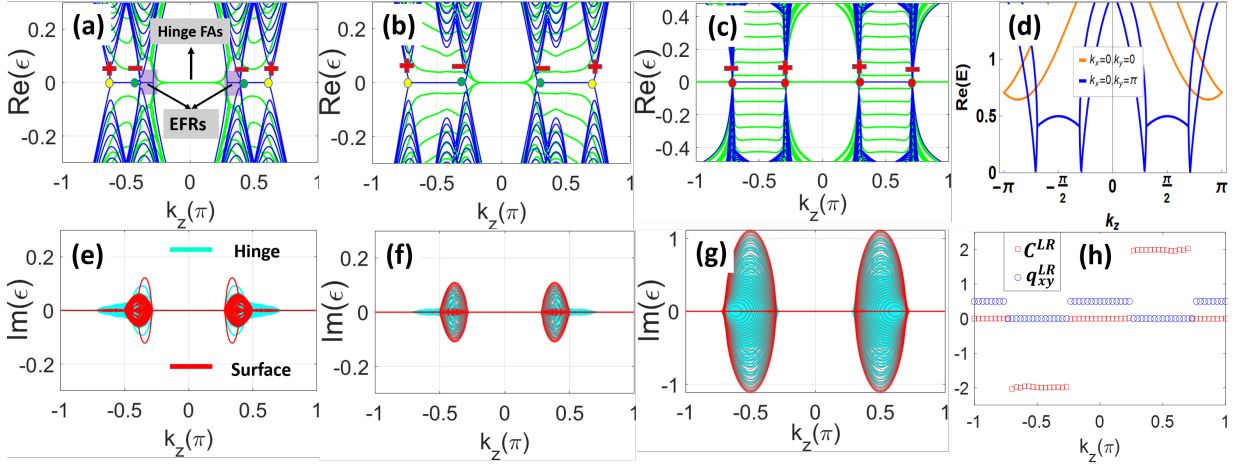
FIG. 3. The real part of spectrum at x-surface [1 OBC] ($k_y = 0$) (blue) and z-hinge [2 OBC] (green) of $H^{\mathcal{T}}$ having (a) $\gamma = -1, m_2 = 0.85, \alpha = 0.3$, (b), $\gamma = -1, m_2 = 0.85, \alpha = 0.6$ (c) $\gamma = 0, m_2 = 0.9, \alpha = 0.5$. (d) The real part of bulk spectrum for (c,g) along k_z for $k_x = k_y = 0$(orange) and $k_x = 0, k_y = \pi$ (blue). (e-g) The imaginary counterparts of (a-c)[red:x-surface, cyan: z-hinge]. (h) The corresponding biorthogonal chern number ($\mathcal{C}^{LR}$, red) and quadrupole momment (q_{xy}^{LR}, blue) of (c,d,g).

we show that the NHWNs can be deformed instantly, upon applying an external Hermitian perturbation. We choose a C_4-symmetric perturbation, $\delta_1 a_0(\mathbf{k})\sigma^3\kappa^0$ as an example and for sake of brevity, we only focus on the inversion symmetric model. Firstly, we note that the δ_1 break the symmetries of $\mathcal{P}AI$ and so gap out the EFRs. More importantly, upon application of δ_1 in the bulk the NHWNs deform to a unique nodal line we call *monopole comet* that preserves the same monopole charge of orig-

FIG. 4. (a) The winding number $\bar{w}_l$ at $k_y = 0$(red) and $k_y = \pi$(blue) planes for $H_w^{\mathcal{I}}$.[$\gamma = -1$, $m_1 = 0.8, \alpha = 0.3$] (b) The real WNs (dashed blue) and C-NHWNs (solid orange) of $H_w^{\mathcal{I}}$ in presence of tilting perturbation $0.8\sin(k_z - pi/2)\mathbb{I}_4$ [$\gamma = -0.6, \alpha = 0.3, m_1 = 0.8$]. (c) The x-surface of $H^{\mathcal{I}}$ in presence of $\delta_1 = 0.05$ showing the deformed NHWNs and gapped EFRs. (d) $H^{\mathcal{I}}$ in presence of $\delta_2 = 0.05$, monopole charges and direction of chiralities are denoted by dots and arrows, respectively (see [53] for plot of Im(E)).

inal NHWNs in Fig. 4(c), but on the surface their corresponding FAs are connected at the original position of NHWNs (i.e, head of comet). This distinct behavior of NHWNs can be used to distinguish them from real stable Hermitian WNs [63].

Exceptional Tilt-Rigidity.— Type-II WSMs have dispersion that is strongly anisotropic around the Weyl nodes such that its slope changes sign along some directions [64]. Interestingly, we find that the C-NHWNs show strong resistance against tilting due to presence of ESs, a phenomenon which we call *Exceptional tilt-rigidity*. Fig. 4(b), shows the real WNs at ($k_x = 0, k_y = 0$) (dashed blue) and NHWNs at ($k_x = 0, k_y = \pi$) (orange) in presence of a tilting perturbation. As is evident for the same amount of tilt strength the C-NHWNs are tilted much lesser compare to the case of real WNs. This is true also in compare to the R-NHWNs. This simple but interesting phenomenon provide an experimental knob for detecting of NHWNs.

Exceptional Helicity.— Now we reveal the intriguing surface instability of EFRs. In the presence of $\delta_2 a_0(\mathbf{k})\sigma^3\kappa^2$, remarkably, the EFRs deform and in doing so the band connectivity of the FAs connecting the WNs is altered. In Fig. 4(d), as a result of δ_2 the two WNs at opposite $\mathbf{k}$ connect to their partner at $-\mathbf{k}$. This lead to the area on the surface having counter-propagating FAs. It is noteworthy that this can not occur in Hermitian WSMs. In order to understand this we note that at $k_y = 0, \pi$ the x-surface respects the anti-PT symmetry which then enforces that a band with energy E to be paired with a band with energy $-E^*$. Therefore, the helical FAs with different Im(E) cannot gap out each other in the real part of energy. We refer to this intrinsically non-Hermitian phenomena as *exceptional helicity*.

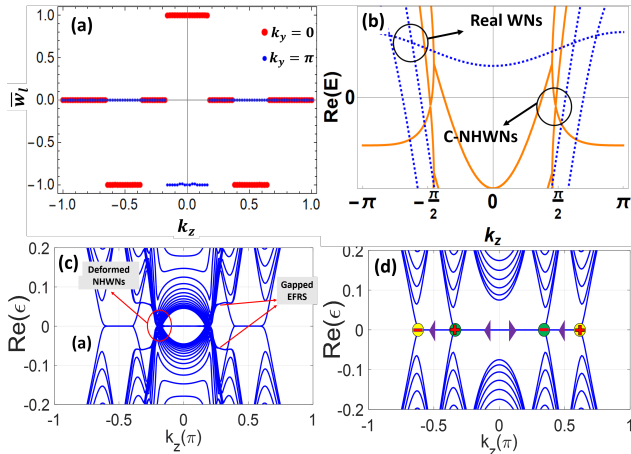*Experimental remarks.—* The 2d quadrupole insula-

tors, which are the building blocks of HOWSM models of our work, have already been realized both in Hermitian [29–32] and non-Hermitian regimes [65, 66]. Moreover, a 3D realization of non-Hermitian topological phases has been demonstrated as well [67]. Recently, Hermitian higher-order semimetals have also been experimentally realized in multiple platforms [68–70]. In particular, Ref.[69], have explicitly simulated the $H^{\mathcal{I}(\mathcal{T})}(m_{1,(2)} = 0)$ model. Therefore, we hope that our results will motivate an experimental realization (specially in electric circuits [32, 67, 69, 71–78]) of non-Hermitian higher-order Weyl semimetals.

Note Added.—During the preparation of this work, another paper appeared on arxiv [79] which discussed a model hosts Weyl exceptional ring (as oppose to this work which presents models having new type of non-Hermitian Weyl nodes). The focus and the physics of two works are very different.

---

* sayedaliakbar.ghorashi@stonybrook.edu

[1] Emil J. Bergholtz, Jan Carl Budich, and Flore K. Kunst, "Exceptional topology of non-hermitian systems," Rev. Mod. Phys. **93**, 015005 (2021).

[2] Yuto Ashida, Zongping Gong, and Masahito Ueda, "Non-hermitian physics," Advances in Physics **69**, 249435 (2020).

[3] Wladimir A Benalcazar, B Andrei Bernevig, and Taylor L Hughes, "Quantized electric multipole insulators." Science **357**, 61–66 (2017).

[4] Wladimir A Benalcazar, B Andrei Bernevig, and Taylor L Hughes, "Selected for a Viewpoint in Physics Electric multipole moments, topological multipole moment pumping, and chiral hinge states in crystalline insulators," Physical Review B **96**, 245115 (2017).

[5] Zhida Song, Zhong Fang, and Chen Fang, "$(d − 2)$-dimensional edge states of rotation symmetry protected topological states," Phys. Rev. Lett. **119**, 246402 (2017).

[6] Zongping Gong, Yuto Ashida, Kohei Kawabata, Kazuaki Takasan, Sho Higashikawa, and Masahito Ueda, "Topological phases of non-hermitian systems," Phys. Rev. X **8**, 031079 (2018).

[7] Kohei Kawabata, Ken Shiozaki, Masahito Ueda, and Masatoshi Sato, "Symmetry and topology in non-hermitian physics," Phys. Rev. X **9**, 041015 (2019).

[8] Fei Song, Shunyu Yao, and Zhong Wang, "Non-hermitian topological invariants in real space," Phys. Rev. Lett. **123**, 246801 (2019).

[9] Flore K. Kunst, Elisabet Edvardsson, Jan Carl Budich, and Emil J. Bergholtz, "Biorthogonal bulk-boundary correspondence in non-hermitian systems," Phys. Rev. Lett. **121**, 026808 (2018).

[10] Kohei Kawabata, Sho Higashikawa, Zongping Gong, Yuto Ashida, and Masahito Ueda, "Topological unification of time-reversal and particle-hole symmetries in non-hermitian physics," Nature Communications **10** (2019), 10.1038/s41467-018-08254-y.

[11] Dan S. Borgnia, Alex Jura Kruchkov, and Robert-Jan Slager, "Non-hermitian boundary modes and topology," Phys. Rev. Lett. **124**, 056802 (2020).

[12] Huitao Shen, Bo Zhen, and Liang Fu, "Topological band theory for non-hermitian hamiltonians," Phys. Rev. Lett. **120**, 146402 (2018).

[13] Daniel Leykam, Konstantin Y. Bliokh, Chunli Huang, Y. D. Chong, and Franco Nori, "Edge modes, degeneracies, and topological numbers in non-hermitian systems," Phys. Rev. Lett. **118**, 040401 (2017).

[14] Nobuyuki Okuma, Kohei Kawabata, Ken Shiozaki, and Masatoshi Sato, "Topological origin of non-hermitian skin effects," Phys. Rev. Lett. **124**, 086801 (2020).

[15] Shunyu Yao and Zhong Wang, "Edge states and topological invariants of non-hermitian systems," Phys. Rev. Lett. **121**, 086803 (2018).

[16] Yi Chen Hu and Taylor L. Hughes, "Absence of topological insulator phases in non-hermitian *pt*-symmetric hamiltonians," Phys. Rev. B **84**, 153101 (2011).

[17] Hengyun Zhou and Jong Yeon Lee, "Periodic table for topological bands with non-hermitian symmetries," Phys. Rev. B **99**, 235112 (2019).

[18] Josias Langbehn, Yang Peng, Luka Trifunovic, Felix von Oppen, and Piet W. Brouwer, "Reflection-symmetric second-order topological insulators and superconductors," Phys. Rev. Lett. **119**, 246401 (2017).

[19] Frank Schindler, Ashley M. Cook, Maia G. Vergniory, Zhijun Wang, Stuart S. P. Parkin, B. Andrei Bernevig, and Titus Neupert, "Higher-order topological insulators," Science Advances **4**, eaat0346 (2018).

[20] Shunyu Yao, Fei Song, and Zhong Wang, "Non-hermitian chern bands," Phys. Rev. Lett. **121**, 136802 (2018).

[21] Sayed Ali Akbar Ghorashi, Xiang Hu, Taylor L. Hughes, and Enrico Rossi, "Second-order dirac superconductors and magnetic field induced majorana hinge modes," Phys. Rev. B **100**, 020509 (2019).

[22] Sayed Ali Akbar Ghorashi, Taylor L. Hughes, and Enrico Rossi, "Vortex and surface phase transitions in superconducting higher-order topological insulators," Phys. Rev. Lett. **125**, 037001 (2020).

[23] Benjamin J. Wieder, Zhijun Wang, Jennifer Cano, Xi Dai, Leslie M. Schoop, Barry Bradlyn, and B. Andrei Bernevig, "Strong and fragile topological dirac semimetals with higher-order fermi arcs," Nature Communications **11** (2020), https://doi.org/10.1038/s41467-020-14443-5.

[24] Zhijun Wang, Benjamin J. Wieder, Jian Li, Binghai Yan, and B. Andrei Bernevig, "Higher-order topology, monopole nodal lines, and the origin of large fermi arcs in transition metal dichalcogenides $x\text{te}_2$ ($x = \text{Mo, W}$)," Phys. Rev. Lett. **123**, 186401 (2019).

[25] Dumitru Călugăru, Vladimir Juričić, and Bitan Roy, "Higher-order topological phases: A general principle of construction," Phys. Rev. B **99**, 041301 (2019).

[26] Tianhe Li, Penghao Zhu, Wladimir A. Benalcazar, and

Taylor L. Hughes, "Fractional disclination charge in two-dimensional C_n-symmetric topological crystalline insulators," Phys. Rev. B **101**, 115115 (2020).

[27] Raquel Queiroz, Ion Cosma Fulga, Nurit Avraham, Haim Beidenkopf, and Jennifer Cano, "Partial lattice defects in higher-order topological insulators," Phys. Rev. Lett. **123**, 266802 (2019).

[28] Bitan Roy, "Antiunitary symmetry protected higher-order topological phases," Phys. Rev. Research **1**, 032048 (2019).

[29] Christopher W. Peterson, Wladimir A. Benalcazar, Taylor L. Hughes, and Gaurav Bahl, "A quantized microwave quadrupole insulator with topologically protected corner states," Nature **555**, 346–350 (2018).

[30] Jiho Noh, Wladimir A. Benalcazar, Sheng Huang, Matthew J. Collins, Kevin P. Chen, Taylor L. Hughes, and Mikael C. Rechtsman, "Topological protection of photonic mid-gap defect modes," Nature Photonics **12**, 408–415 (2018).

[31] Marc Serra-Garcia, Valerio Peri, Roman Süsstrunk, Osama R. Bilal, Tom Larsen, Luis Guillermo Villanueva, and Sebastian D. Huber, "Observation of a phononic quadrupole topological insulator," Nature **555**, 342–345 (2018).

[32] Stefan Imhof, Christian Berger, Florian Bayer, Johannes Brehm, Laurens W. Molenkamp, Tobias Kiessling, Frank Schindler, Ching Hua Lee, Martin Greiter, Titus Neupert, and Ronny Thomale, "Topolectrical-circuit realization of topological corner modes," Nature Physics **14**, 925–929 (2018).

[33] Haoran Xue, Yahui Yang, Fei Gao, Yidong Chong, and Baile Zhang, "Acoustic higher-order topological insulator on a kagome lattice," Nature materials **18**, 108–112 (2019).

[34] Kunal Shastri and Francesco Monticone, "Dissipation-induced topological transitions in continuous weyl materials," Phys. Rev. Research **2**, 033065 (2020).

[35] Yong Xu, Sheng-Tao Wang, and L.-M. Duan, "Weyl exceptional rings in a three-dimensional dissipative cold atomic gas," Phys. Rev. Lett. **118**, 045701 (2017).

[36] Kohei Kawabata, Masatoshi Sato, and Ken Shiozaki, "Higher-order non-hermitian skin effect," Phys. Rev. B **102**, 205118 (2020).

[37] Tao Liu, Yu-Ran Zhang, Qing Ai, Zongping Gong, Kohei Kawabata, Masahito Ueda, and Franco Nori, "Second-order topological phases in non-hermitian systems," Phys. Rev. Lett. **122**, 076801 (2019).

[38] Elisabet Edvardsson, Flore K. Kunst, and Emil J. Bergholtz, "Non-hermitian extensions of higher-order topological phases and their biorthogonal bulk-boundary correspondence," Phys. Rev. B **99**, 081302 (2019).

[39] Yongxu Fu, Jihan Hu, and Shaolong Wan, "Non-hermitian second-order skin and topological modes," Phys. Rev. B **103**, 045420 (2021).

[40] Ryo Okugawa, Ryo Takahashi, and Kazuki Yokomizo, "Second-order topological non-hermitian skin effects," Phys. Rev. B **102**, 241202 (2020).

[41] Zhiwang Zhang, María Rosendo López, Ying Cheng, Xiaojun Liu, and Johan Christensen, "Non-hermitian sonic second-order topological insulator," Phys. Rev. Lett. **122**, 195501 (2019).

[42] María Rosendo López, Zhiwang Zhang, Daniel Torrent, and Johan Christensen, "Multiple scattering theory of non-hermitian sonic second-order topological insulators,"

[43] Jiaxin Pan and Longwen Zhou, "Non-hermitian floquet second order topological insulators in periodically quenched lattices," Phys. Rev. B **102**, 094305 (2020).

[44] Hong Wu, Bao-Qin Wang, and Jun-Hong An, "Floquet second-order topological insulators in non-hermitian systems," Phys. Rev. B **103**, L041115 (2021).

[45] Xi-Wang Luo and Chuanwei Zhang, "Higher-order topological corner states induced by gain and loss," Phys. Rev. Lett. **123**, 073601 (2019).

[46] Jien Wu, Xueqin Huang, Jiuyang Lu, Ying Wu, Weiyin Deng, Feng Li, and Zhengyou Liu, "Observation of corner states in second-order topological electric circuits," Phys. Rev. B **102**, 104109 (2020).

[47] Xingping Zhou, Jing Wu, and Yongfeng Wu, "Topological corner states in non-hermitian photonic crystals," Optics Communications **466**, 125653 (2020).

[48] Ching Hua Lee, Linhu Li, and Jiangbin Gong, "Hybrid higher-order skin-topological modes in nonreciprocal systems," Phys. Rev. Lett. **123**, 016805 (2019).

[49] Motohiko Ezawa, "Non-hermitian higher-order topological states in nonreciprocal and reciprocal systems with their electric-circuit realization," Phys. Rev. B **99**, 201411 (2019).

[50] Sayed Ali Akbar Ghorashi, Tianhe Li, Masatoshi Sato, and Taylor L. Hughes, "Non-hermitian higher-order dirac semimetals," (2021), arXiv:2106.14914 [cond-mat.mes-hall].

[51] Sayed Ali Akbar Ghorashi, Tianhe Li, and Taylor L. Hughes, "Higher-order weyl semimetals," Phys. Rev. Lett. **125**, 266804 (2020).

[52] Kohei Kawabata, Takumi Bessho, and Masatoshi Sato, "Classification of exceptional points and non-hermitian topological semimetals," Phys. Rev. Lett. **123**, 066405 (2019).

[53] Supplementary material.

[54] Mao Lin and Taylor L. Hughes, "Topological quadrupolar semimetals," Phys. Rev. B **98**, 241103 (2018).

[55] Alexander Cerjan, Meng Xiao, Luqi Yuan, and Shanhui Fan, "Effects of non-hermitian perturbations on weyl hamiltonians with arbitrary topological charges," Phys. Rev. B **97**, 075128 (2018).

[56] In this case the NHWNs which appear are of type R-NHWNs. There are alternatives to Fig. 2. We can instead fix the α and tune m_1, which then the C-NHWNs would appear. Note that the general trend particularly the Fig. 2(a,b and d) can occur and only details of surface phase transitions from b-d could differ.In [53], we have shown one alternative example. Also, We note that unlike the $\alpha = 0$ limit of [50] the surface states become complex only when bulk is complex as well. ().

[57] Because of $\mathcal{T}\mathcal{M}_y\mathcal{M}_z$, one can show that $\det H(k_y, k_z)$ is real, and it is non-zero except on the exceptional ring. Then $\mathrm{sgn}[\det H(k_y, k_z)]$ gives the $\mathbb{Z}_2$ topological number ().

[58] $q_{x,y} = \frac{1}{2\pi} \mathrm{Im} \left[\ln \langle \Psi^{R(L)} | \hat{U}_{x,y} | \Psi^{R(L)} \rangle \right]$, where $\hat{U}_{x,y} = e^{2i\pi \sum_r r_x r_y \hat{n}_r / (L_x L_y)}$, $|\Psi^{R(L)}\rangle = \prod_{n \in occ} \gamma^\dagger_{n,R(L)} |0\rangle$, $\Psi^{R(L)}$ denote the right and left eigenvecors and x (N_x) and y (N_y) are the coordinate operator (sample size) along x and y directions, respectively. ().

[59] William A. Wheeler, Lucas K. Wagner, and Taylor L. Hughes, "Many-body electric multipole operators in ex-

Communications Physics **2**, 1–7 (2019).

tended systems," Phys. Rev. B **100**, 245135 (2019).

[60] Byungmin Kang, Ken Shiozaki, and Gil Young Cho, "Many-body order parameters for multipoles in solids," Phys. Rev. B **100**, 245134 (2019).

[61] Seishiro Ono, Luka Trifunovic, and Haruki Watanabe, "Difficulties in operator-based formulation of the bulk quadrupole moment," Phys. Rev. B **100**, 245133 (2019).

[62] $\mathcal{C} = \frac{2\pi i}{L_x' L_y'} \text{Tr}' \left(\mathcal{P}_\alpha \left[[x, \mathcal{P}_\alpha], [y, \mathcal{P}_\alpha] \right] \right)$, $\mathcal{P}_\alpha = \sum_{n \in \alpha} |nR\rangle\langle nL|$, $L_{x,y}'$ are the bulk size of a fully bounded lattice and the trace Tr' sums over the inner area (i.e. we can remove $l_{x,y}$ unit cells from the edge such that $L_{x(y)}' = L_{x(y)} - l_{x(y)}$) ().

[63] The δ_1 gaps out the EFRs with opposite signs and then induces hinge domain walls, resulting a $\mathcal{I}$-NHHOWSM having surface FAs and hinge states. Similarly, one can use the C_4-breaking version of these perturbations as $\delta_{1,2}' \sigma^3 \kappa^{0,2}$ (see [53]). We did not find a significant difference in terms of bulk nodes and surface. However, breaking C_4 will gap out the hinge FAs in $H^\mathcal{T}$. ().

[64] N. P. Armitage, E. J. Mele, and Ashvin Vishwanath, "Weyl and dirac semimetals in three-dimensional solids," Rev. Mod. Phys. **90**, 015001 (2018).

[65] He Gao, Haoran Xue, Zhongming Gu, Tuo Liu, Jie Zhu, and Baile Zhang, "Non-hermitian route to higher-order topology in an acoustic crystal," Nature Communications **12** (2021), 10.1038/s41467-021-22223-y.

[66] Zhiwang Zhang, María Rosendo López, Ying Cheng, Xiaojun Liu, and Johan Christensen, "Non-hermitian sonic second-order topological insulator," Phys. Rev. Lett. **122**, 195501 (2019).

[67] Deyuan Zou, Tian Chen, Wenjing He, Jiacheng Bao, Ching Hua Lee, Houjun Sun, and Xiangdong Zhang, "Observation of hybrid higher-order skin-topological effect in non-hermitian topolectrical circuits," (2021), arXiv:2104.11260 [cond-mat.mes-hall].

[68] Qiang Wei, Xuewei Zhang, Weiyin Deng, Jiuyang Lu, Xueqin Huang, Mou Yan, Gang Chen, Zhengyou Liu, and Suotang Jia, "Higher-order topological semimetal in acoustic crystals," Nature Materials (2021), 10.1038/s41563-021-00933-4.

[69] Xiang Ni and Andrea Alù, "Higher-order topolectrical semimetal realized via synthetic gauge fields," APL Photonics **6**, 050802 (2021).

[70] Li Luo, Hai-Xiao Wang, Zhi-Kang Lin, Bin Jiang, Ying Wu, Feng Li, and Jian-Hua Jiang, "Observation of a phononic higher-order weyl semimetal," Nature Materials **20**, 794–799 (2021).

[71] Tobias Helbig, Tobias Hofmann, Ching Hua Lee, Ronny Thomale, Stefan Imhof, Laurens W. Molenkamp, and Tobias Kiessling, "Band structure engineering and reconstruction in electric circuit networks," Phys. Rev. B **99**, 161114 (2019).

[72] Tobias Hofmann, Tobias Helbig, Ching Hua Lee, Martin Greiter, and Ronny Thomale, "Chiral voltage propagation and calibration in a topolectrical chern circuit," Phys. Rev. Lett. **122**, 247702 (2019).

[73] Motohiko Ezawa, "Electric circuits for non-hermitian chern insulators," Phys. Rev. B **100**, 081401 (2019).

[74] Ching Hua Lee, Stefan Imhof, Christian Berger, Florian Bayer, Johannes Brehm, Laurens W Molenkamp, Tobias Kiessling, and Ronny Thomale, "Topolectrical circuits," Communications Physics **1**, 1–9 (2018).

[75] Tobias Hofmann, Tobias Helbig, Frank Schindler, Nora Salgo, Marta Brzezińska, Martin Greiter, Tobias Kiessling, David Wolf, Achim Vollhardt, Anton Kabaši, Ching Hua Lee, Ante Bilušić, Ronny Thomale, and Titus Neupert, "Reciprocal skin effect and its realization in a topolectrical circuit," Phys. Rev. Research **2**, 023265 (2020).

[76] Junkai Dong, Vladimir Juričić, and Bitan Roy, "Topolectric circuits: Theory and construction," Phys. Rev. Research **3**, 023056 (2021).

[77] SM Rafi-Ul-Islam, Zhuo Bin Siu, and Mansoor BA Jalil, "Topoelectrical circuit realization of a weyl semimetal heterojunction," Communications Physics **3**, 1–11 (2020).

[78] Rujiang Li, Bo Lv, Huibin Tao, Jinhui Shi, Yidong Chong, Baile Zhang, and Hongsheng Chen, "Ideal type-ii weyl points in topological circuits," National Science Review **8**, nwaa192 (2021).

[79] Tao Liu, James Jun He, Zhongmin Yang, and Franco Nori, "Higher-order weyl-exceptional-ring semimetals," (2021), arXiv:2104.07335 [cond-mat.mes-hall].